Histone Variant macroH2A1.1 Enhances Nonhomologous End Joining-dependent DNA Double-strand-break Repair and Reprogramming Efficiency of Human iPSCs

Sebastiano Giallongo, Daniela eháková, Tommaso Biagini, Oriana Lo Re, Priyanka Raina, Gabriela Lochmanová, Zbynk Zdráhal, Igor Resnick, Pille Pata, Illar Pata, Martin Mistrík, João Pedro de Magalhães, Tommaso Mazza, Irena Koutná, Manlio Vinciguerra

Stem Cells, 2022, **40**, 35–48
https://doi.org/10.1093/stmcls/sxab004
Advance access publication 19 January 2022
Original Research

Histone Variant macroH2A1.1 Enhances Nonhomologous End Joining-dependent DNA Double-strand-break Repair and Reprogramming Efficiency of Human iPSCs

Sebastiano Giallongo[1,2], Daniela Řeháková[1], Tommaso Biagini[3], Oriana Lo Re[1,4], Priyanka Raina[5], Gabriela Lochmanová[6], Zbyněk Zdráhal[6,7], Igor Resnick[4,8,9], Pille Pata[10,11], Illar Pata[10], Martin Mistrík[12], João Pedro de Magalhães[5], Tommaso Mazza[4], Irena Koutná[1,13], Manlio Vinciguerra[1,4,*]

[1]International Clinical Research Center, St. Anne's University Hospital, Brno, Czech Republic
[2]Department of Biology, Faculty of Medicine, Masaryk University, Brno, Czech Republic
[3]Laboratory of Bioinformatics, Fondazione IRCCS Casa Sollievo della Sofferenza, San Giovanni Rotondo, Italy
[4]Department of Translational Stem Cell Biology, Research Institute of the Medical University of Varna (RIMUV), Varna, Bulgaria
[5]Integrative Genomics of Ageing Group, Institute of Ageing and Chronic Disease, University of Liverpool, Liverpool, UK
[6]Central European Institute of Technology, Masaryk University, Brno, Czech Republic
[7]National Centre for Biomolecular Research, Masaryk University, Brno, Czech Republic
[8]Program for Hematology, Immunology, BMT and Cell therapy, St. Marina University Hospital, Varna, Bulgaria
[9]Department of Medical Genetics, Medical University of Varna, Varna, Bulgaria
[10]Department of Chemistry and Biotechnology, Tallinn University of Technology, Tallinn, Estonia
[11]IVEX Lab, Akadeemia 15, Tallinn, Estonia
[12]Laboratory of Genome Integrity, Institute of Molecular and Translational Medicine, Faculty of Medicine and Dentistry, Palacky University, Olomouc, Czech Republic
[13]Department of Histology and Embryology, Faculty of Medicine, Masaryk University, Brno, Czech Republic

*Corresponding author: Manlio Vinciguerra, PhD, International Clinical Research Center (FNUSA-ICRC), Pekarska 53, 656 91, Brno, Czech Republic. Email: manlio.vinciguerra@fnusa.cz

Abstract

DNA damage repair (DDR) is a safeguard for genome integrity maintenance. Increasing DDR efficiency could increase the yield of induced pluripotent stem cells (iPSC) upon reprogramming from somatic cells. The epigenetic mechanisms governing DDR during iPSC reprogramming are not completely understood. Our goal was to evaluate the splicing isoforms of histone variant macroH2A1, macroH2A1.1, and macroH2A1.2, as potential regulators of DDR during iPSC reprogramming. GFP-Trap one-step isolation of mtagGFP-macroH2A1.1 or mtagGFP-macroH2A1.2 fusion proteins from overexpressing human cell lines, followed by liquid chromatography-tandem mass spectrometry analysis, uncovered macroH2A1.1 exclusive interaction with Poly-ADP Ribose Polymerase 1 (PARP1) and X-ray cross-complementing protein 1 (XRCC1). MacroH2A1.1 overexpression in U2OS-GFP reporter cells enhanced specifically nonhomologous end joining (NHEJ) repair pathway, while macroH2A1.1 knock-out (KO) mice showed an impaired DDR capacity. The exclusive interaction of macroH2A1.1, but not macroH2A1.2, with PARP1/XRCC1, was confirmed in human umbilical vein endothelial cells (HUVEC) undergoing reprogramming into iPSC through episomal vectors. In HUVEC, macroH2A1.1 overexpression activated transcriptional programs that enhanced DDR and reprogramming. Consistently, macroH2A1.1 but not macroH2A1.2 overexpression improved iPSC reprogramming. We propose the macroH2A1 splicing isoform macroH2A1.1 as a promising epigenetic target to improve iPSC genome stability and therapeutic potential.

Key words: macroH2A1.1; DNA damage; cell reprogramming; induced pluripotent stem cells.

Received: 4 June 2021; Accepted: 2 September 2021.

Graphical Abstract

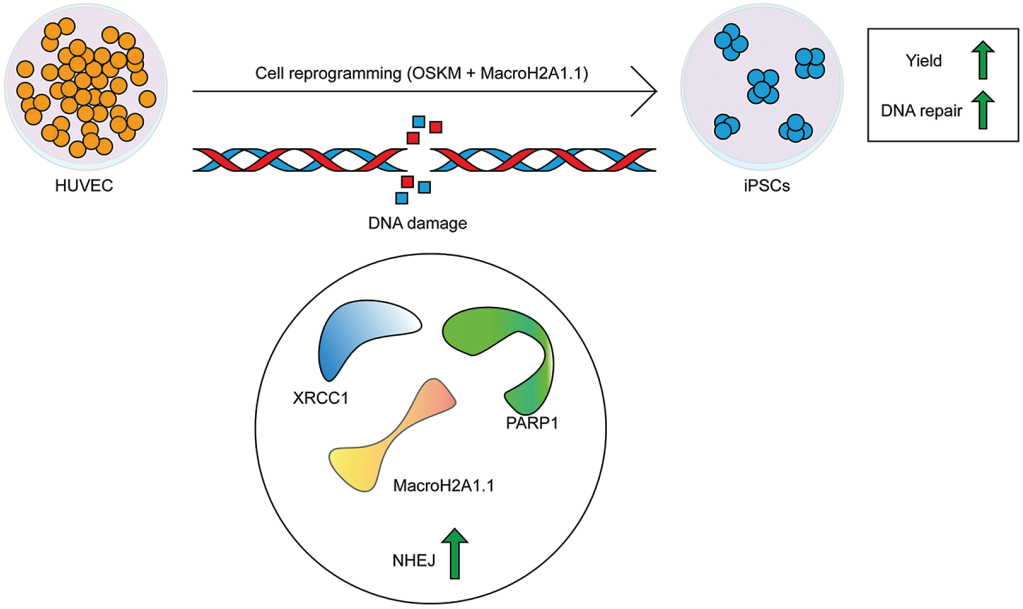

DNA damage repair (DDR) is a safeguard for genome integrity maintenance. Increasing DDR efficiency increases the yield of induced pluripotent stem cells (iPSC) upon OSKM-mediated reprogramming from somatic cells. Histone variant macroH2A1.1, but not its sister alternatively spliced isoform macroH2A1.2, increases the efficiency of iPSC reprogramming by interacting with PARP1 and XRCC1 and activating an NHEJ-dependent DDR pathway.

Significance Statement

Histone macroH2A1 splicing variants macroH2A1.1 and macroH2A1.2 differ for a few amino acids but can have remarkably different roles in cancer pathogenesis and cell differentiation. Reprogramming of somatic cells into iPSC requires oxidative stress and the hyperactivation of DNA damage repair (DDR) pathways: the exact function of macroH2A1 proteins in this process is unknown. The authors found that macroH2A1.1 exclusively interacts with 2 DDR factors as PARP1 and XRCC1, effectors of nonhomologous end-joining (NHEJ) DDR. As consequence, macroH2A1.1 overexpression in vitro boosts NHEJ while its depletion in vivo impairs mice DDR machinery. The authors describe as well the significance of this newly identified macroH2A1.1-dependent NHEJ activation in improving the efficiency of human umbilical vein endothelial cells (HUVEC) reprogramming into iPSC.

Introduction

Genome stability is essential for cellular homeostasis and tumor suppression.[1] During the cell cycle, chromatin undergoes major changes to allow for DNA replication and cell division. The large heterogeneity of DNA-lesion types needs several ad hoc DDR mechanisms[2]: (1) Mismatch repair (MMR), triggered by DNA mismatches and insertion/deletion loops arising from DNA replication; (2) Base excision repair (BER) and single-strand break repair (SSBR), triggered by abnormal DNA bases, simple base-adducts, SSBs generated as BER intermediates or by oxidative damage; (3) Nucleotide excision repair (NER), triggered by lesions that disrupt the DNA double-helix, such as UV photo-products; (4) nonhomologous end joining (NHEJ), triggered by radiation- or chemically induced double-strand breaks (DSBs) plus V(D)J recombination, class-switch recombination (CSR) intermediates; (5) Homologous recombination (HR, including Break-induced replication [BIR]), triggered by DSBs or SSBs (the latter occurs in the case of BIR), stalled replication forks and inter-strand DNA cross-links.[2] DDR defects cause cancers, neurodegenerative diseases, and accelerated aging.[2,3]

The discovery of the induced pluripotent stem cells (iPSC) technology opened a great potential in autologous-based regenerative medicine.[4] While iPSCs are currently used in personalized disease modeling, they are not deemed safe for transplant because of inherent iatrogenic tumorigenesis.[5] There are multiple potential mechanisms for tumorigenicity during induction of pluripotency in somatic cells, all linked to DNA mutations and (epi)genome instability.[5] NHEJ, HR, BER, MMR, and NER have been found to be involved in iPSC reprogramming, with an enhanced although more heterogenous DNA repair activity compared to somatic cells.[6,7] DDR pathways can be considered error-free (ie, HR) or error-prone (ie, NHEJ), depending on the context.[8] Thus, an inefficient repair can result in the introduction of mutations during iPSC reprogramming.[9]

The process of reprogramming implicates a complete remodeling of the somatic epigenetic memory, replaced by new iPSC-specific epigenetic profiles. Epigenetic alterations include DNA methylation, post-translational histone modifications, the substitution of canonical histones with histone variants, and the activity of chromatin remodeling complexes.[10] How to manipulate these epigenetic changes to help efficient iPSC generation is of great clinical interest.

MacroH2A proteins are histone variants coded by 2 distinct genes: H2AFY for macroH2A1, ubiquitous, and H2AFY2 for macroH2A2. While macroH2A1 is expressed ubiquitously, macroH2A2 expression is restricted only to few tissues.

MacroH2A1 and macroH2A2 are composed of a domain sharing 66% homology with the histone H2A, and they are unique due to their peculiar conformation, in which a C-terminal linker brings together the histone domain to a domain called macrodomain.[11-13] MacroH2A1 displays 2 isoforms resulting from alternative exon splicing: macroH2A1.1 and macroH2A1.2, having common and distinct biological and pathological roles.[11-15] MacroH2A1 is significantly enriched in differentiated cells but expressed at low levels upon iPSC reprogramming,[16,17] forming a barrier against pluripotency. In turn, macroH2A1 depletion not only improved cell differentiation, but it also allowed differentiated cells to return to a stemness condition.[16,17]

Distinct splice variant-specific functions of the macroH2A1.1 and macroH2A1.2 gene products occur in the frame of DDR pathways. MacroH2A1.1 has been associated with PARP1-dependent DNA repair, being recruited to sites of DNA damage via its poly-(ADP-ribose) (PAR) binding domain.[14] MacroH2A1.2, lacking the ability to bind PAR, has also been implicated in DNA repair, protecting fragile genomic sites through its recruitment by the histone chaperone ATRX.[18-20] In particular, macroH2A1.1 is physically associated with Poly ADP-ribose polymerase 1 (PARP1) and Ku heterodimer (Ku70/Ku80),[21] main components of the NHEJ repair pathway, while macroH2A1.2 seems to promote HR during replicative stress.[19] However, whether macroH2A1.1 and macroH2A1.2 isoforms modulate DDR pathways during iPSC reprogramming is unknown. In this work, we investigated whether macroH2A1 splice variants could differently orchestrate 2 key aspects of iPSC function: genome maintenance and efficiency of reprogramming.

Material and Methods

Cell Culture, GFP-Trap, and Mass Spectrometry

Parental HepG2 cells (ATCC) were cultured in high glucose DMEM (1×) supplemented with 10% fetal bovine serum (FBS), 1% penicillin/streptomycin. MacroH2A1.1-mtagGFP and macroH2A1.2-mtagGFP overexpression in HepG2 cells was induced through lentiviral infection, as previously described.[22,23] U2OS-GFP reporter cell lines were previously described.[24] Isolation of macroH2A1.1-mtagGFP and macroH2A1.2-mtagGFP using GFP-Trap Magnetic Agarose Kit (#gtmak-20, ChromoTek, Munich, Germany) was described earlier.[25] Before immunoaffinity enrichment, the samples were incubated with binding control magnetic agarose beads to remove nonspecifically bound proteins. Cells with an empty mtagGFP vector were used as a control of unspecific binding to GFP protein. Each sample type (ie, macroH2A1.1-mtagGFP, macroH2A1.2-mtagGFP, and mtagGFP) was represented by 4 biological replicates. LC-MS/MS analysis was performed as previously described.[26,27] Detailed description of sample preparation (ie, immunoaffinity enrichment and on-bead enzymatic digestion) followed by proteomic analysis (LC-MS/MS, database search, and data evaluation) are provided in the Supplementary Material. Proteins with fold change expression values ≥ 5.0 and adjusted *P*-value ≤ .01 between mtagGFP (control) and macroH2A1-mtagGFP isoforms overexpressing cells were considered as potential binding partners.

Immunoblotting Analyses

Immunoblotting was performed as previously described.[23] Primary rabbit antibodies against XRCC1 (#2735), H2A (#2572), γ-H2AX (#9718), macroH2A1.1 (#12455), macroH2A1.2 (#4827S), and PFK-PT (#13045) were purchased from Cell Signalling Technology (Massachusetts, USA). Rabbit antibody against PARP1 (ab227244) and c-Myc (ab201780) and mouse antibody against XRCC5 (ab119935) were obtained from Abcam (Cambridge, UK). Secondary antibody anti-rabbit HRP-linked (#7074) and anti-mouse HRP-linked (#7076) were obtained from Cell Signalling Technology (Massachusetts, USA).

Reporter Cell Lines

U2OS-GFP reporter cells were transfected as already described.[24] Plasmid preparation, transient transfection, production of lentiviruses, and generation of mCer3 stable cell lines are described in the Supplementary Material.

MacroH2A1.1 Knock-out Mice

MacroH2A1.1 knock-out (KO, or $^{-/-}$) was achieved as previously described.[28] Briefly, a 12 Kb fragment of the murine H2AFY sequence was subcloned into p15A-HSV tk-DTA-amp from a BAC. The intron among exons 6a and 6b were modified to carry a lacZ-neo cassette,[29] flanked by loxP and rox sites at the 5′ and 3′ ends. Moreover, a rox site was inserted upstream of exon 6a, while another loxP site was inserted downstream of exon 6b. Cre/loxP recombination removes exon 6b and the lacZ-neo cassette, resulting in macroH2A1.1 depletion with this design. Targeting of macroH2A1.1 was validated using southern-blot analysis.[28] The construct was inserted in A9 ES cells using electroporation. The cells were then injected in C57BL/6 8 cell-stage embryos. MacroH2A1$^{fl/fl}$ mice were crossed with HPRT-Cre mice (129S1/Sv-Hprttm1(CAG-cre)Mnn/J), purchased from Jackson Laboratories, USA, obtaining heterozygous macroH2A1.1$^{fl/-}$ mice. Further crossing of these mice with deleter HPRT-Cre mice generated macroH2A1.1$^{-/-}$. For survival experiments, total body irradiation was administered to macroH2A1$^{fl/fl}$, macroH2A1$^{fl/-}$, and macroH2A1$^{-/-}$ mice (n = 25-30 per group), restrained in holders, using an MK-1-68A Cesium-137 Gamma animal irradiator (J.L. Shepherd and Associates) (California, USA), with 1000 rad in a single dose. After irradiation, all animals were returned to the animal facility. Mice were bred and maintained at Plaisant Srl (Rome, Italy), in accordance with current Italian legislation (article 9, 27 January 1992, number 116) under a license from the Italian Health Ministry.

Histology and Immunohistochemistry

Excised livers were fixed in 4% paraformaldehyde solution, dehydrated in serial alcohol solutions, embedded in paraffin, cut into 5-µm-thick sections stained with Hematoxylin and Eosin (H&E) and examined under a light microscope (Nikon, Tokyo, Japan).[30] Phosphorylation of the histone protein H2AX (γH2AX) was used as DSB indicator using immunohistochemistry. Primary antibody against γH2AX (ab26350) was purchased from Abcam (Cambridge, UK). Immunohistochemistry protocol for mice livers and semi-quantitative evaluation was previously described.[31,32]

Mouse embryonic Fibroblasts

Primary mouse embryonic fibroblasts (MEFs) were derived from macroH2A1.1$^{Fl/Fl}$ or macroH2A1.1$^{-/-}$ embryos as previously described.[33] For irradiation experiments (1000 rad), only MEFs of early passages (1-3) were utilized. Cell viability/

proliferation was assessed by MTT assay as previously described.[34]

Flow Cytometry

Flow cytometry analysis was performed using BD Biosciences FACSCanto.[35] U2OS-GFP reporter cells were harvested and centrifugated at 350×*g*, 5 minutes, 24°C. Cells were then washed 3 times with PBS and finally resuspended in 100 µL of FACS buffer (PBS, 1% FBS) for flow cytometry analysis.

HUVEC Reprogramming and iPSC Differentiation

Human umbilical vein endothelial cells (HUVECs, Thermo Fisher Scientific, Massachusetts, USA) were cultured in Nunc EasYFlasks in Endothelial Cell Growth medium 2 (Promocell, Heidelberg, Germania). Cells were collected by TrypLE express enzyme (Thermo Fisher Scientific, Massachusetts, USA) according to the manufacturer's instructions. Epi5 Episomal iPSC Reprogramming Kit (Thermo Fisher Scientific, Massachusetts, USA) was used for reprogramming in combination with Neon Transfection System 10 µL Kit. Shortly, 10^5 living cells in 10 µL R buffer were prepared and 1 µL of the content of each vial from the reprogramming kit was added. Where applicable, 1 µg of plasmids expressing macroH2A1.1-6His or macroH2A1.2-6His were added (Addgene, Massachusetts, USA).[36] Neon Transfection tube was filled with 3 mL E buffer and cells with plasmid were electroporated with Pulse voltage 1400 V, Pulse Width 20 ms, Pulse number 2. Cells were seeded on hESC-qualified MatriGel coated cell culture treated 35 mm Petri dishes in endothelial medium, which was changed daily until day 5, when it was exchanged for mTeSR. To establish cell lines, individual clones were picked mechanically and cultured on hESC-qualified MatriGel (Corning, New York, USA) in mTeSR 1. The subsequent passaging method was EDTA dissociation to clumps with ROCKi supplementation (Y-27632 2HCl, Selleckchem, Texas, USA). All media were supplemented with ZellShield (Minerva Biolabs). iPSCs differentiation was examined using Human Pluripotent Stem Cell Functional Identification Kit purchased from R&D System (#SC027B) (Minnesota, USA), following the manufacturer protocol and using secondary anti-goat Alexa488-linked (A11055). After differentiation, cells were screened through flow cytometry using BD Biosciences FACSCanto.[35] For alkaline poshpatase (AP) staining, cells were rinsed twice with PBS, fixed in cold 4% paraformaldehyde in PBS for 10 minutes, and rinsed twice with PBS before 1 mL of Alkaline phosphatase mix (AB0100) (Sigma-Aldrich, Missouri, USA) was added to each well of a 6-well plate. The plate was placed in the dark and analyzed after 15 minutes. Results were analyzed using ImageJ (Maryland, USA).

Immunofluorescence

Cells were processed for immunofluorescence, as we previously described.[37-39] Primary rabbit antibodies against XRCC1 (#2735) (#13045) and γH2Ax (#9718) were purchased from Cell Signalling Technology (Massachusetts, USA). Rabbit antibodies against PARP1 (ab227244) and 6-His-TAG (ab18184) were obtained from Abcam (Cambridge, UK). Secondary antibody anti-rabbit Alexa555-linked (A11035) and anti-mouse Alexa647-linked (A21236) were obtained from Thermo Fisher Scientific (Massachusetts, USA). Secondary antibody HRP goat-anti-rabbit (ab6721) was purchased from Abcam (Cambridge, UK). EdU staining was performed as already described.[40] Images were acquired using Leica TCS SP8X at 63× magnification. Results were analyzed using ImageJ (Maryland, USA).

RNA-Seq and Co-expression Network Analysis

Samples were prepared for RNA-Seq and analyzed as already described.[23] Work pipeline and the co-expression analysis are described in the Supplementary Material.

Statistical Analyses

Data are shown as means ± Standard error of the mean (SEM). Group comparison was assessed using Student's test, using GraphPad Prism Software (version 5.00 for Windows, San Diego, CA, USA): significance was $P \leq .05$.

Results

Identification of macroH2A1.1 and macroH2A1.2 Binding Partners by Mass Spectrometry-based Proteomics

To identify specific macroH2A1.1 and macroH2A1.2 interacting partners, the proteins were stably overexpressed as mtagGFP-tagged proteins in human HepG2 hepatoma cells.[22,41] MacroH2A1.1-mtagGFP and macroH2A1.2-mtagGFP fusion proteins were isolated using GFP-Trap,[42] consisting of an anti-GFP Nanobody/V_{HH} coupled to magnetic agarose beads, and processed for mass spectrometry analysis. MacroH2A1.1, but not macroH2A1.2, interacted with PARP1, as previously reported,[43] and with X-ray repair cross-complementing protein 1 (XRCC1), a newly identified partner (FC > 10; *P*-adj ≤ .001) (Supplementary Table 1). Other top interacting partners, binding to both macroH2A1 splicing isoforms, included X-ray repair cross-complementing protein 5 (XRCC5), Disco-interacting protein 2 homolog B (DIP2B), ATP-dependent 6-phosphofructokinase, platelet type (PFKP), Ras GTPase-activating protein-binding protein 2, and Histone H2B type 1-J (FC > 10; *P*-adj ≤ .001; Supplementary Table 1). Using a cut-off of FC > 5 (*P*-adj ≤ .01), 56 and 41 enriched binding proteins were identified by mass spectrometry in macroH2A1.1 and macroH2A1.2 overexpressing cells, respectively. Known associations between binding histones and DNA-repair proteins with macroH2A1.1 or macroH2A1.2 were inferred and represented using STRING (Fig. 1A,B, respectively). The full list of macroH2A1.1-mtagGFP and macroH2A1.2-mtagGFP interacting proteins is found in Supplementary Data 1 and 2. Mass spectrometric results were confirmed using a biochemical approach. We performed immunoprecipitation of macroH2A1.1-mtagGFP and macroH2A1.2-mtagGFP with GFP-Trap in HepG2 cells, to validate protein-protein interaction through immunoblotting analysis (Fig. 1C). We were able to confirm XRCC5 and PFKP as macroH2A1.1 and macroH2A1.2 common interacting partners, while PARP1 and XRCC1 were physically associated only with macroH2A1.1 (Fig. 1C).

Distinct Effects of macroH2A1.1 and macroH2A1.2 on NHEJ DNA Repair Outcome

PARP1 and XRCC1, which we identified as exclusive binding partners of macroH2A1.1, have been implicated in NHEJ.[44-47] NHEJ effectors Ku70/Ku80 have been recently identified at the crossroad between DNA damage repair pathways

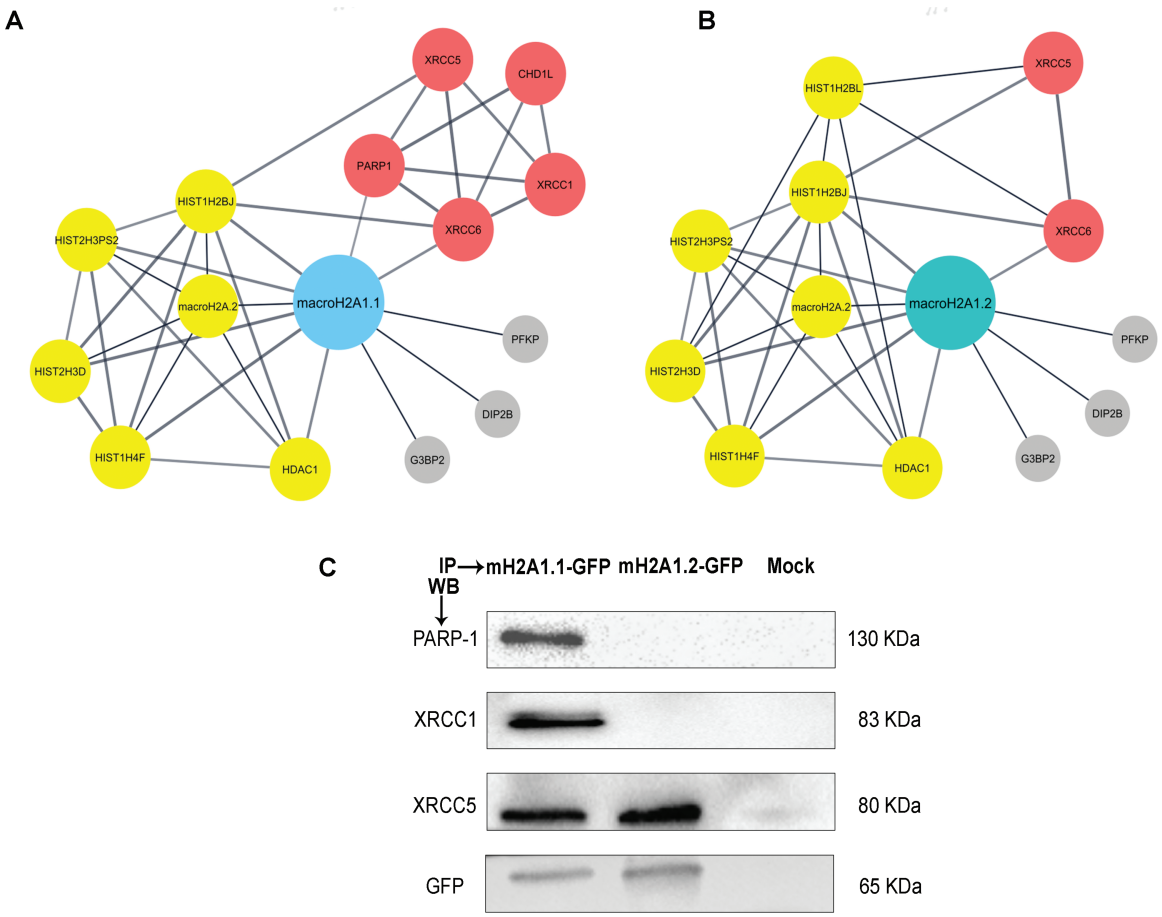

Figure 1. Interacting networks for macroH2A1.1 (**A**) and macroH2A1.2 (**B**) splicing isoforms created in STRING database based on the significantly enriched proteins in proteomic analysis (FC > 5; adjusted $P \leq .01$). The visualization was done using Cytoscape. Histones (yellow nodes) and DNA-repair proteins (red nodes) were connected by STRING at minimum required interaction score of 0.7 (high confidence). Other proteins, identified with high confidence by mass spectrometry, were added to the network as potential interacting partners (ie, G3BP2, DIP2B, and PFKP; gray nodes). (**C**) Immunoblot analysis of macroH2A1.1 and macroH2A1.2 binding partners in HepG2 cells. For immunoprecipitations negative controls, mock rabbit IgG were used. XRCC5 was confirmed as common interacting partner for macroH2A1 splicing isoforms. PARP1 and XRCC1 are interacting exclusively with macroH2A1.1. A representative image of 3 independent experiments is shown.

mediated by NHEJ and BER.[48] Moreover, macroH2A1.1 but not macroH2A1.2 physically associates with Ku70/Ku80.[21] To elucidate the epigenetic role of macroH2A1 isoforms on the activity of the NHEJ pathway, we transiently introduced macroH2A1.1 and macroH2A1.2 as mCer3-tagged proteins into the U2OS-GFP NHEJ reporter cell line, hosting a cassette harboring a GFP inactive site inside their genome[24] (Fig. 2A). We ectopically expressed I-SceI, a site-specific endonuclease recognizing a sequence located inside the cassette, triggering the DNA damage response,[24] by transient transfection. Cells were processed for flow cytometry 48 hours after co-transfection of macroH2A1.1-mCer3, or macroH2A1.2-mCer3 (Supplementary Fig. 1A), and I-SceI. To evaluate the effect of macroH2A1 isoforms on DDR, we gated and analyzed double-positive mCer3-GFP populations (Supplementary Fig. 2). As a positive control, we silenced the expression of BRCA2: abrogation of this tumor suppressor has been reported to enhance NHEJ occurrence[49] (Supplementary Fig. 1B). With regards to the total NHEJ pathway, macroH2A1 isoforms behaved differently in the U2OS model: transient transfection of macroH2A1.1-mCer3 increased the activation of this DDR pathway ($P < .01$), while macroH2A1.2-mCer3 impaired it ($P < .05$), compared to control cells (Fig. 2B, left panel). We were able to confirm the latter findings by stable overexpression of mCer3-tagged macroH2A1 isoforms via lentiviral transduction in U2OS-GFP reporter cells for NHEJ: in this setting macroH2A1.1-mCer3 enhanced NHEJ activity, in a more profound manner compared to transient transfection ($P < 0.0001$; Fig. 2B, right panel). On the other hand, macroH2A1.2-mCer3 stable overexpression did not affect the NHEJ pathway (Fig. 2B, left panel).

To analyze the functional interplay between macroH2A1.1, PARP1, and XRCC1, we silenced PARP1 and/or XRCC1 protein expression using siRNA in U2OS-GFP reporter cells for NHEJ, which were transiently overexpressing macroH2A1.1 or macroH2A1.2 (Supplementary Fig. 1C). We achieved a ~50% downregulation for both PARP1 and XRCC1 protein expression levels (Supplementary Fig. 1D). Silencing of BRCA2 was used again as a positive control. In control U2OS-GFP reporter cells for NHEJ, silencing of PARP1, XRCC1 or both, did not elicit effects on NHEJ occurrence (Fig. 2C, left panel), Interestingly, in macroH2A1.1-overexpressing U2OS-GFP reporter cells for NHEJ, silencing of PARP1 or XRCC1, or both, slightly attenuated the observed macroH2A1.1-dependent

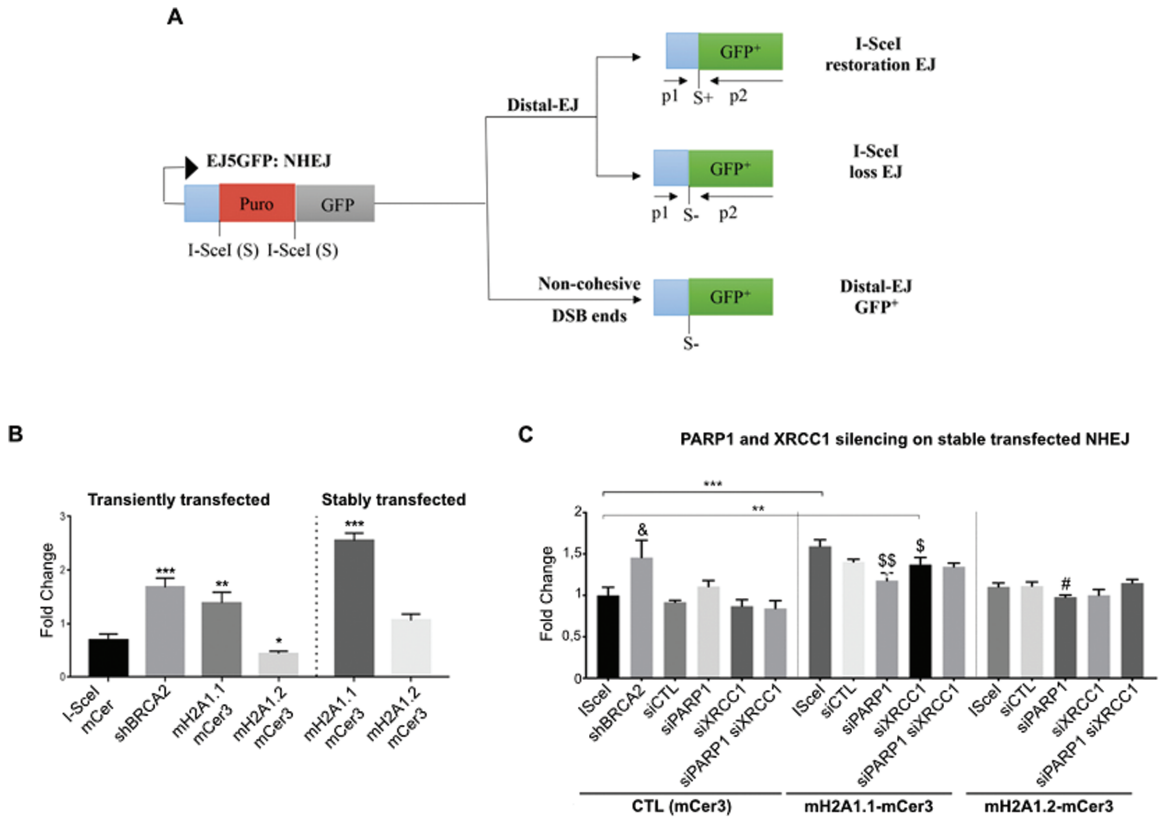

Figure 2. Flow cytometry analysis to investigate the effect of macroH2A1.1 and macroH2A1.2 on NHEJ pathways. U2OS-GFP for NHEJ were used as cell model. (**A**). Diagram showing the construct designed to investigate the occurrence of NHEJ after the repair of the DNA damage triggered by I-SceI ectopic expression.[24] MacroH2A1 splicing isoforms were transiently and stably overexpressed in U2OS-GFP reporter cells as mCer3- tag proteins (**B**). Effect of PARP1 and XRCC1 silencing on NHEJ reporter U2OS stably overexpressing mCer3 alone (left panel), macroH2A1.1-mCer3 (middle panel) or macroH2A1.2-mCer3 (right panel) tagged proteins. For control of PARP1 and/or XRCC1 silencing, a scramble siRNA (siCTL) was used (**C**). Data are normalized to control mCer3 stably expressing cells, transiently transfected with I-SceI (I-SceI/mCer3). * ($P \leq .05$ relative to I-SceI/mCer3); ** ($P \leq .01$ relative to I-SceI scramble-mCer3); *** ($P \leq .001$ relative to I-SceI/mCer3); **** ($P \leq .0001$ relative to I-SceI/mCer3); & ($P \leq .05$ relative to I-SceI/mCer3); $ ($P \leq .05$ relative to I-SceI/mH2A1.1-mCer3); $$ ($P \leq .01$ relative to I-SceI/mH2A1.1-mCer3); # ($P \leq .05$ relative to I-SceI/mH2A1.2-mCer3). Data are presented as means ± SEM; $n = 3$.

increase in NHEJ occurrence (Fig. 2C, middle panel). In macroH2A1.2-overexpressing U2OS-GFP reporter cells, no activation of NHEJ was observed under any condition; PARP1 silencing triggered a slight decrease in the basal levels of NHEJ activity (Fig. 2C, right panel). Taken together, these results highlight a specific role of macroH2A1.1 in activating NHEJ.

MacroH2A1.1 Knock Out Impairs DNA Repair in Mice

MacroH2A1.1 involvement in NHEJ prompted us to analyze the role of these splicing isoforms in vivo. We thus irradiated with a systemic dose of 1000 rad, routinely used to induce extensive DNA damage, bone marrow cell depletion, and death within few weeks, wild type (macroH2A1.1$^{fl/fl}$, $n = 30$), heterozygous (macroH2A1.1$^{fl/-}$, $n = 27$), and knock-out (macroH2A1.1$^{-/-}$, $n = 25$) mice, which we have previously generated through the Cre/LoxP system.[28] Strikingly, a statistically significant ($P = .0384$) decrease in survival was observed in macroH2A1.1$^{-/-}$) mice (~50% lethality) compared to macroH2A1.1$^{fl/-}$ and macroH2A1.1$^{-/-}$ littermates (~25%-30% lethality) (Fig. 3A). Because acute irradiation induces liver injury, livers from surviving macroH2A1.1$^{-/-}$mice were examined 20 days post-irradiation (1000 rad). The livers displayed congested blood vessels with prominent hemorrhage and hepatocytes with altered morphology reminiscent of steatohepatitis-like damage; these features were much milder or absent in the livers of irradiated matched macroH2A1.1$^{fl/fl}$ mice (Fig. 3B). Phosphorylation of H2A.x on S139 (γH2A.x) is directly related to the amount of DNA damage experienced by the cells.[49] Immunohistochemical analysis revealed increased nuclear positivity for γH2A.x staining in the livers of irradiated macroH2A1.1$^{-/-}$ mice compared to macroH2A1.1$^{fl/fl}$ littermates (Fig. 3B). Consistent with these findings, in vitro irradiation (1000 rad) of primary mouse embryonic fibroblasts (MEFs) derived from macroH2A1.1$^{-/-}$ embryos showed decreased cell viability compared to naive macroH2A1.1$^{fl/fl}$ (Fig. 3C), which was accompanied by increased γH2A.x expression (Fig. 3D). Overall, these data support the conclusion that the histone variant macroH2A1.1 is required for optimal DDR and repair upon irradiation in vivo and ex vivo.

MacroH2A1.1 Interacts with NHEJ Effectors During HUVEC Reprogramming Into iPSC

During the reprogramming process toward pluripotency, cells experience a large amount of DNA damage as a consequence of reactive oxygen species (ROS) production.[12] As a result, several mutations are generated, increasing the risk for the adverse tumorigenic potential of iPSC.[11] We investigated the role of macroH2A1.1 and macroH2A1.2 in DDR modulation upon iPSC reprogramming. Although macroH2A proteins have generally been described as barriers against pluripotency,[16] the role of macroH2A1 splicing variants has not been investigated. To

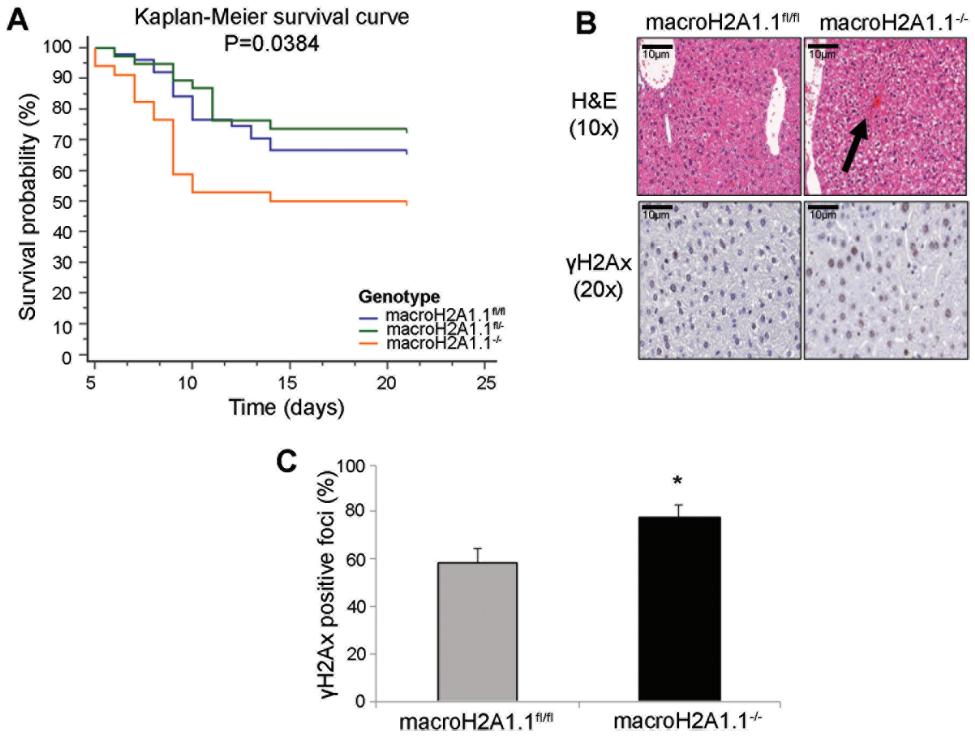

Figure 3. DDR investigation on wild type (macroH2A1.1$^{fl/fl}$), heterozygous (macroH2A1.1$^{fl/-}$) and knock-out (macroH2A1.1$^{-/-}$) mice. (**A**) Kaplan-Meier survival curve of mice post-irradiation (P = .0384 compared to macroH2A1.1$^{fl/fl}$), (n = 25-30 mice/group). Survivals of mice were closely monitored several times per day. (**B**) Upper panels: representative histological sections of livers from irradiated mice, processed for H&E staining upon sacrifice; magnification 10×. Lower panels: immunohistochemistry staining for γH2A.x on liver sections from irradiated mice. Representative images are shown (left, magnification 20×), together with semi-quantitative evaluations of frequency of staining positivity (right). * (P < .05, relative to macroH2A1.1$^{fl/fl}$). (**C**) Primary MEFs obtained from macroH2A1.1$^{fl/fl}$ and macroH2A1.1$^{-/-}$, cultured at early passage (1-3) were irradiated or not (no IR) with 1000 rad. Forty-eight hours after irradiation, proliferation/viability was assessed by MTT assay. (**D**) In parallel, cell lysates from MEFs were processed for immunoblotting with an γH2A.x antibody. Representative images are shown in the left panels. Histone H2A was used as a loading control. N = 5. *** (P < .001 relative to macroH2A1.1$^{fl/fl}$ no IR), ### (P < .001 relative to macroH2A1.1$^{fl/fl}$ 1000 rad).

this aim, macroH2A1.1 and macroH2A1.2 were transiently overexpressed as 6-His-tagged proteins in HUVEC together with an episome construct inducing Oct4, Sox2, Lin28, Klf4, and L-Myc expression, in turn inducing reprogramming into iPSC.[50] Overexpression of macroH2A1 isoforms was monitored using the 6-His-Tag in signal super-resolution confocal microscopy (Fig. 4 and Supplementary Fig. 3). Compared to control cells carrying the reprogramming episome, imaging data analysis showed a peak of macroH2A1 isoforms expression on the fourth day of the reprogramming process (P < .0001; Fig. 4A). Therefore, we decided to examine the effects of macroH2A1 isoforms expression on the early stages of cell reprogramming. To confirm the data obtained in HepG2 cells, we analyzed the colocalization of macroH2A1 isoforms with PARP1 and XRCC1 in HUVEC undergoing reprogramming (Fig. 4 and Supplementary Fig. 3). MacroH2A1.1, but not macroH2A1.2, signal display significantly increased colocalization with PARP1 (P < .0001; Fig. 4B,C). XRCC1 signal also display significantly increased colocalization with macroH2A1.1, compared to with macroH2A1.2 (P < .0001, Fig. 4D,E). Interestingly, XRCC1 and PARP1 signals showed an enhanced colocalization after macroH2A1.1 transient overexpression, compared to macroH2A1.2 (P < .0001) and control cells carrying only the reprogramming episome (P < .05; Supplementary Fig. 3A,B). Moreover, we sought to investigate macroH2A1.1 and macroH2A1.2 roles in cell proliferation, which is tightly related to the modulation of DDR.[51] For this purpose, HUVEC on the fourth day of reprogramming were analyzed for 5-Ethynyl-2′-deoxyuridine (EdU) staining (Supplementary Fig. 3C-E). Compared to macroH2A1.2 (P < .001) and control cells (P < .001), macroH2A1.1 transient overexpression increased cell proliferation in HUVEC undergoing reprogramming (Supplementary Fig. 3D). Moreover, the EdU signal was significantly colocalized with macroH2A1.1, but not with macroH2A1.2 (P < .0001, Supplementary Fig. 3E). Taken together, our imaging analyses demonstrate that macroH2A1.1, but not its sister molecule macroH2A1.2, closely colocalizes with XRCC1 and PARP1 and enhances cell proliferation in the early stages of reprogramming.

MacroH2A1.1 Boosts DDR and Reprogramming Transcriptional Patterns During HUVEC Reprogramming Into iPSC

As in HUVEC undergoing reprogramming macroH2A1.1 may interact with the DNA repair effector proteins XRCC1 and PARP1, we then asked whether genes associated with a modulation of DDR responses could be affected in HUVEC undergoing reprogramming. To this aim, we performed RNA-Seq analysis on HUVEC cells upon macroH2A1.1 and macroH2A1.2 overexpression. We conducted an unbiased analysis comparing the transcriptome of HUVEC carrying just the reprogramming episomes (control, CTL) with HUVEC in addition overexpressing macroH2A1.1 or macroH2A1.2, at the fourth day of reprogramming, as in the previous experiments. Altogether, 1004 differentially expressed genes (DEGs) were found between macroH2A1.1 and CTL HUVEC cells, and 1172 DEG were found between HUVEC cells overexpressing

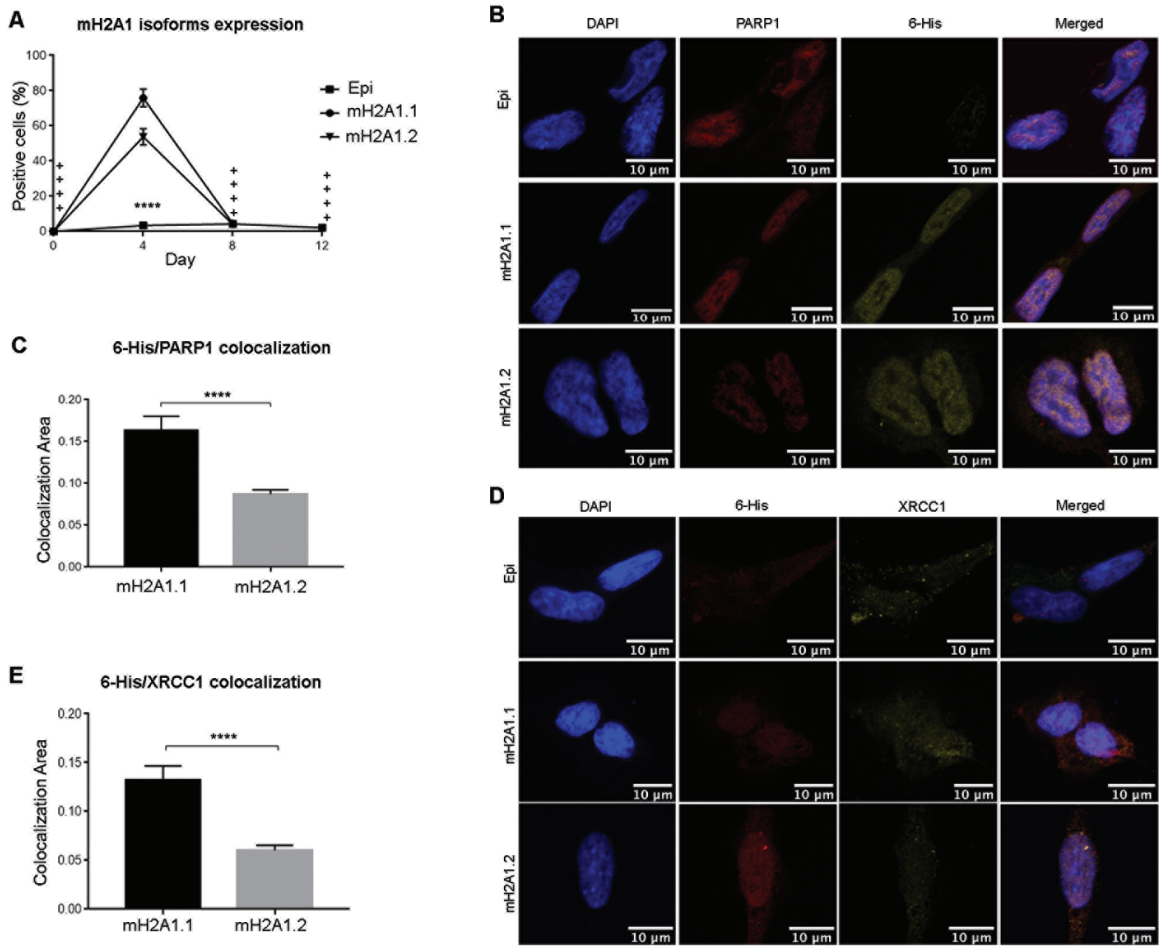

Figure 4. MacroH2A1 isoforms' role in Huvec reprogramming. Expression analysis of macroH2A1.1 and macroH2A1.2 along cell reprogramming (**A**). Data are reported as percentage of cells positive for macroH2A1.1 and macroH2A1.2 staining. **** ($P \leq .0001$ relative to reprogramming episomes cells). ++++ ($P \leq 0.0001$ relative to macroH2A1.1 and macroH2A1.2 cells on the fourth day of reprogramming). Super-resolution confocal microscopy analysis of macroH2A1.1, macroH2A1.2, and PARP1 in HUVEC on the fourth day of reprogramming (**B**). Colocalization analysis of macroH2A1 isoforms and PARP1 signals (**C**). Data are reported as colocalization area of the signals. **** ($P \leq .0001$). Super resolution confocal microscopy analysis of macroH2A1.1, macroH2A1.2, and XRCC1 in HUVEC on the fourth day of reprogramming (**D**). Colocalization analysis of macroH2A1 isoforms and XRCC1 signals (**E**). Data are reported as colocalization area of the signals. **** ($P \leq .0001$). All the data are presented as means ± SEM; $n = 4$.

macroH2A1.1 and macroH2A1.2. Of note, 242 genes were differentially expressed in macroH2A1.2 versus CTL HUVEC cells. The 3 conditions also showed a negligible transcriptional overlap, consisting of 2 genes only (Fig. 5A). Interestingly, either macroH2A1.1 or macroH2A1.2 isoforms overexpression triggered transcriptional fold changes (FC) of DDR DEG with higher frequencies for low-fold inductions (Supplementary Fig. 4). We first conducted targeted analyses: intersecting the list of genes known to contribute to the DDR biological process according to the Ingenuity Pathway Analysis (IPA) knowledgebase (Supplementary Data 3) with the list of DEG in each experimental condition, we obtained a consensus of 44 genes. Figure 5B shows that the transcriptional patterns of these genes in macroH2A1.1-overexpressing HUVEC cells were markedly different than macroH2A1.2-overexpressing HUVEC cells and CTL HUVEC cells undergoing reprogramming. Conversely, the transcriptional profiles related to DDR were more similar between macroH2A1.2-overexpressing versus CTL HUVEC cells undergoing reprogramming (Fig. 5B). An IPA analysis inclusive of all DEG implicated in DDR processes showed that there were robust and overlapping networks involved in the DDR processes that were differently regulated when macroH2A1.1 was overexpressed (Fig. 5C). On the other hand, macroH2A1.2 overexpression was involved in a smaller network formed by DEGs connected to DDR (Fig. 5D). We next asked whether macroH2A1.1 could also affect the expression of genes involved in cell reprogramming. We thus intersected a list of genes known in IPA to be involved in the cell reprogramming process with that of the DEG in each experimental condition and obtained 12 consensus genes. MacroH2A1.1 overexpression affected the transcription pattern of genes involved in cell reprogramming. The transcriptional pattern of this gene set in macroH2A1.2- overexpressing HUVEC was similar to CTL HUVEC cells (Supplementary Fig. 5A). As a result of macroH2A1.1 overexpression, CHAF1A, KLF4, SOX2, and POU5F1 mRNA levels were decreased, while c-Myc gene expression was increased (Supplementary Fig 5B). On the other hand, SOX2 and POU5F1 were the only genes downregulated by macroH2A1.2 overexpression (Supplementary Fig. 5C). c-Myc upregulation in macroH2A1.1- but not macroH2A1.2-overexpressing HUVEC was also confirmed at the protein level, and it was accompanied also by a similar upregulation of Oct4, Nanog, and Sox2 reprogramming factors (Supplementary Fig. 5D). Therefore, our

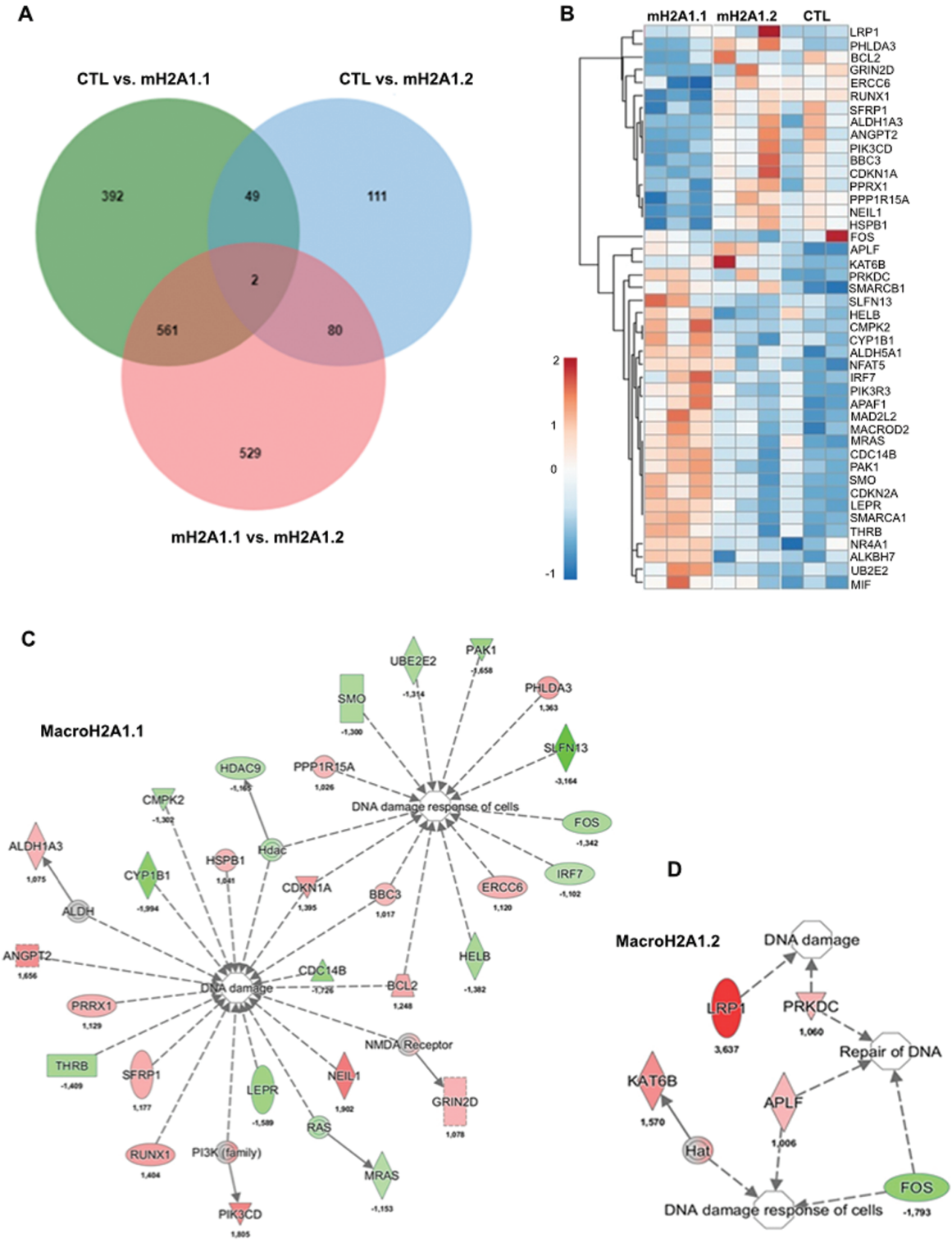

Figure 5. Venn diagram of DEGs when comparing HUVEC CTL, mH2A1.1, and macroH2A1.2 (**A**). CTL versus macroH2A1.1 comparison showed that 1004 genes were differently affected. Compared to macroH2A1.2, macroH2A1.1 differently affected 1172 genes. Two hundred and forty-two genes were differently regulated in macroH2A1.2 versus CTL HUVEC. Only 2 genes showed a transcriptional overlap among the 3 conditions. For differential expression, a cut-off of 2-folds for FC and a $P \leq .05$ were considered. Heatmap representing 44 genes participating to DDR according to IPA (**B**). The transcriptional profile of macroH2A1.1 showed an overall enhancement of the DDR compared to macroH2A1.2 and CTL. Representation of IPA networks wiring DEGs that participate to the DDR biological process in macroH2A1.1 (**C**) and macroH2A1.2 (**D**). Differentially expressed genes are here identified with different colors: light to dark red indicates increasing expression, while light to dark green indicates decreasing expression. Solid or dashed lines state direct or indirect relationships between genes, respectively.

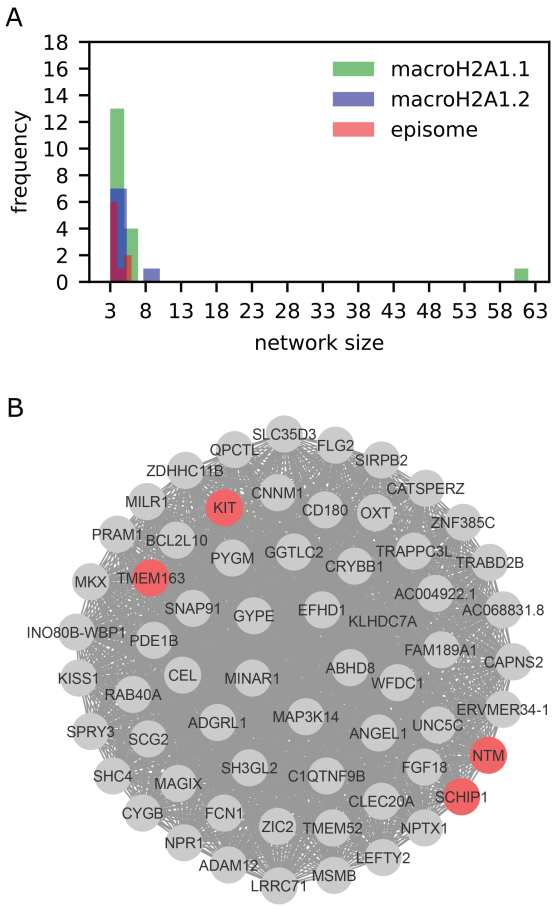

Figure 6. Frequency plot of genes sorted by cluster sizes (**A**). macroH2A1.1 cluster of size 62 containing TMEM163, NTM, SCHIP1, and KIT (**B**). All genes colored in red are downregulated in macroH2A1.1 compared with control cells (Epi).

targeted bioinformatics analyses showed that macroH2A1.1, and to a less extent macroH2A1.2, modulated DDR and reprogramming gene expression during HUVEC reprogramming into iPSC.

Next, we performed an unbiased gene co-expression network analysis, an approach that has proven effective at assigning putative functions to genes based on the functional annotation of their co-expressed partners.[52] The network of control (Epi) cells wired 5831 genes with 16836 edges, measuring an average clustering coefficient of 0.322, network completeness of 0.001, and 2208 clusters of genes. The macroH2A1.2-overexpression dependent network contained 5851 genes linked with 17793 edges and characterized by an average clustering coefficient of 0.355, network completeness of 0.001, and 2154 clusters of genes. The macroH2A1.1-overexpression dependent network contained 7183 genes linked with 23151 edges and characterized by an average clustering coefficient of 0.364, network completeness of 0.012, and 2615 clusters of genes. Hence, we found that both macroH2A1.1 and macroH2A1.2 networks were more connected than the control (Epi) network, with the former exhibiting the highest clustering coefficient and completeness scores. Both macroH2A1.1 and macroH2A1.2 counted several genes involved in small-sized clusters (Fig. 6A). MacroH2A1.1 overexpression led to a better-organized network grouped in one large cluster composed of 62 genes, which are likely involved in common biological functions (Fig. 6B). Of note, TMEM163 (FC = 2.98, *P*-value = .01), NTM (FC = 3.73, *P*-value = .0002), SCHIP1 (FC = 2.38, *P*-value = .0003), and KIT (FC = 3.52, *P*-value = .0004) were DEG significantly downregulated in macroH2A1.1 compared to control cells. These effectors are all involved in neuronal function and differentiation.[53-56]

MacroH2A1.1 Improves the Yield of HUVEC Reprogramming Into iPSC, But Not Their Differentiation Potential

Full reprogramming of cells can be established starting from 12 days after the transfection with the reprogramming episomes.[50,57] In this context, AP overexpression is one of the main markers associated with stemness acquisition, since this protein is overexpressed in embryonic stem cells.[58] We thus decided to probe the reprogramming efficiency of HUVEC overexpressing macroH2A1 splicing isoforms, performing AP staining 12 days after transfection. Results showed that macroH2A1.1, but not macroH2A1.2, overexpression increased the number of iPSC colonies compared to CTL cells ($P < .05$; Fig. 7A,B), consistent with the increased proliferation demonstrated by Edu staining observed at the fourth day of reprogramming (Supplementary Fig. 3). iPSCs can be ideally differentiated into any cell type.[12] We thus examined the ability of iPSCs, generated while overexpressing macroH2A1 isoforms, to differentiate into mesoderm, endoderm, and ectoderm. The efficiency of differentiation was assessed through flow cytometry, measuring the expression of Brachyury, Sox17, and Otx2, differentiation markers for mesoderm, endoderm, and ectoderm, respectively. Cells were stained using a GFP-coupled secondary antibody. Differentiated cells were thus gated as GFP$^+$ population (Supplementary Fig. 6). Results showed that overexpression of macroH2A1.1 or macroH2A1.2 did not affect iPSCs differentiation into mesoderm and endoderm, while there was a preferential disadvantage of macroH2A1.1- over macroH2A1.2-overexpressing cells to give rise to ectoderm (Fig. 7C). Taken together, our results showed that, compared to control and macroH2A1.2 counterpart, macroH2A1.1 overexpression can increase the yield of iPSC colonies generated upon the reprogramming process, and to bias the latter toward an impaired neurogenic commitment.

Discussion

Since their discovery in 2006, iPSC potential to differentiate in any cell line represented a great promise for the development of personalized medicine and the production of engineered tissues.[59,60] However, since the first tests on nude mice, iPSC triggered the formation of teratoma, discouraging their clinical application.[60] One of the main factors linked to iPSC tumorigenicity is the accumulation of genetic aberrations during the reprogramming process.[60] The enhancement of DDR pathways may thus result in the production of fully safe iPSC for clinical applications. The modulation of a particular DNA repair pathway depends on several factors, including epigenetic alterations like DNA methylation, post-translational histone modifications, and the substitution of canonical histones with histone variants.[10] The 2 exon splicing variants of histone variant macroH2A1, macroH2A1.1, and macroH2A1.2, differ

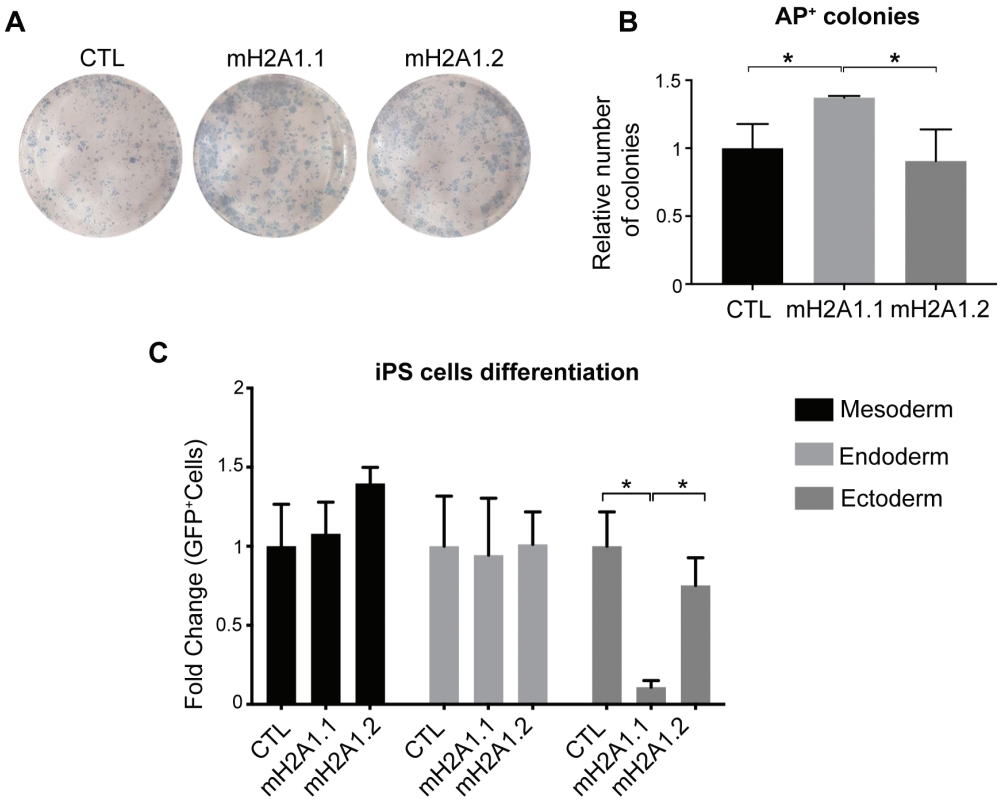

Figure 7. Representative images showing CTL, macroH2A1.1, and macroH2A1.2 AP+ induced pluripotent stem cells (iPSC) colonies (**A**). Quantification of AP+ iPSC colonies (**B**). Data are reported as relative number of colonies. * ($P \leq .05$ relative to CTL and macroH2A1.2). Results are representative of 4 separate experiments and are normalized on reprogramming episomes. Histogram showing the differentiation ability of iPSC (**C**). Data are reported as relative amount of CTL cells. Results are representative of 3 separate experiments and are normalized on reprogramming episomes. All the results are reported as means ± SEM.

in a small region included in the C-terminal macrodomain, conferring to the 2 splicing isoforms peculiar features.[11,61] MacroH2A1.1 can bind ADP-ribose moieties, thus interacting with PAR polymers synthesized by PARP1, and with PARP1 itself.[21,43,62] MacroH2A1.2, on the other hand, accumulates at genomic fragile regions promoting HR, mainly interacting with BRCA1.[20,63,64] We hypothesized that elucidating macroH2A1 isoforms individual interactomes could represent a viable strategy to dissect their respective roles in distinct DDR. By performing LC-MS/MS analysis in human HepG2 cells overexpressing either macroH2A1.1 or macroH2A1.2 tagged with GFP,[22] we were able to confirm the reported macroH2A1.1-PARP1 interaction.[21,62] Moreover, we uncovered for the first time that XRCC1 is a macroH2A1.1 exclusive interacting protein. When overexpressed as mCer3-tag proteins in U2OS-GFP reporter cells, macroH2A1.1 enhanced NHEJ occurrence, while macroH2A1.2 inhibited this DDR pathway. Consistently, both PARP1 and XRCC1, exclusive binding partners of macroH2A1.1, are known to promote NHEJ.[65,66] PARP1 is recruited to DNA damages sites and catalyzes the synthesis of PAR polymers, serving as a scaffold for the recruitment of DNA repair effector proteins.[66] Interestingly, PARP1 operates also in an NHEJ-backup pathway dependent on DNA ligase IIIα activity, competing with the canonical NHEJ pathway carried out by the KU complex.[65] This pathway, still poorly characterized, relies on XRCC1 activity as well.[66] In this work, we showed for the first time evidence that macroH2A1.1, potentially as a consequence of its interaction with PARP1 and XRCC1, promotes the NHEJ pathway in vitro. Mirroring these data our in vivo and ex vivo analyses using macroH2A1.1 KO mice showed that these animals were more sensitive to irradiation compared to their wild-type counterparts. Interestingly, both liver sections and MEFs obtained from mice displayed high levels of γH2A.x-positive foci, reflecting an increased amount of DNA DSB upon macroH2A1.1 loss. Also, it was shown that mice devoid of all macroH2A proteins (macroH2A1.1/macroH2A1.2/macroH2A2) exhibited impaired intestinal regeneration upon irradiation,[67] suggesting a dominant effect for macroH2A1.1 in modulating systemic DDR pathways upon genotoxic insults, independent of the presence or absence of other macroH2A proteins. DDR has a fundamental role in somatic cells undergoing reprogramming: corroborating the interactome data obtained in HepG2 cells, super-resolution confocal microscopy imaging confirmed macroH2A1.1 interaction with PARP1 and XRCC1 also in HUVEC undergoing reprogramming into iPSC. In addition to its role in DNA repair, PARP1 hyperactivation may trigger apoptosis as a consequence of increased DNA damage: in this context, macroH2A1.1 stabilizes PAR polymers, resulting in enhanced cell survival.[62] These findings are consistent with our data on macroH2A1.1 overexpressing HUVEC displaying an increased number of EdU positive proliferating cells in the S-phase of the cell cycle.[68] Both PARP1 and XRCC1 are important factors for DNA replication, during the ligation of Okazaki fragments.[69] Unligated Okazaki fragments are normally detected as single-strand DNA breaks and resolved through DDR mechanism FEN1-dependent or through PARP1/XRCC1-dependent mechanisms.[69] Upon reprogramming into

iPSC, our transcriptomic data showed that while macroH2A1.2-overexpressing and control HUVEC displayed a similar profile of DEG, macroH2A1.1-overexpressing HUVEC displayed a significantly larger number of DEG involved in DDR pathways. Accordingly, IPA analysis inclusive of the DEG showed that several families of genes involved in DNA repair were differently regulated by macroH2A1.1, while only few pathways were affected by macroH2A1.2. Of note, for both macroH2A1 splicing isoforms, the FC of DDR DEG with higher frequencies showed low-fold inductions. This might suggest that macroH2A1 isoforms contribute to a low-energy solution to regulatory responses.[70,71] The macroH2A family, including macroH2A2, has been reported to behave as an epigenetic barrier toward the acquisition of cell pluripotency.[16] Our data show for the first time that macroH2A1.1 overexpression selectively enhanced DEG related to pluripotency acquisition. On the other hand, macroH2A1.2-overexpressing and control HUVEC showed a comparable transcriptional profile. Accordingly, we speculate that macroH2A2 and macroH2A1.2, but not macroH2A1.1, could be the macroH2A family members responsible for reprogramming inhibition. In agreement with the finding that macroH2A1.1 is an enhancer of DNA repair and cell reprogramming, we reported that the number of iPSC colonies increased upon macroH2A1.1, but not macroH2A1.2, overexpression. However, while macroH2A1.2 does not seem to impact iPSC differentiation into the 3 major embryonic germ layers (endoderm, mesoderm, and ectoderm), which is consistent with previous reports,[16] macroH2A1.1-overexpressing reprogrammed iPSC have a decreased potential to generate the ectoderm. Interestingly, mRNA levels of *H2AFY*, coding for macroH2A1, are upregulated in tissues of patients affected by Huntington's disease,[72] and Huntington's disease human embryonic stem cells present ectodermal anomalies during development.[73] The alternative splicing event generating macroH2A1 variants is regulated by RNA helicases Ddx5 and Ddx7.[71] Interestingly, siRNA-mediated depletion of both Ddx5 and Ddx7 improves the expression of macroH2A1.1, decreasing macroH2A1.2, in tumorigenic contexts.[71] Notably, Ddx5 silencing in MEFs improves the efficiency of iPSC reprogramming.[74] The family of mRNA binding proteins Quaking (QKIs), has also been reported as a macroH2A1 alternative splicing regulator.[75] In particular, QKI5 has been recently linked to promote macroH2A1.1 expression impairing macroH2A1.2 production.[76] Interestingly, ectopic overexpression of QKI5 has been recently reported to promote endothelial cells differentiation from human iPSC mediating angiogenesis and neovascularization through Vascularization Endothelial Growth Factor Receptor 2 (VEGFR2) activation.[77] Harnessing QKI5 activity could thus represent an alternative strategy to enhance macroH2A1.1 expression to improve iPSC production and availability for clinical trials. Currently, the most promising clinical trials employing iPSC are ongoing for ophthalmologic purposes,[78] for the treatment of acute graft versus host disease/GvHD,[79] and for the treatment of Parkinson's and heart diseases,[80,81] and for other disorders.[60] However, undifferentiated cells retained in the final cell product, together with maintenance of reprogramming factors and genetic mutations still represent the main obstacle for iPSC application in regenerative medicine.[60] In conclusion, we report for the first time that histone variant macroH2A1 splicing isoform macroH2A1.1, but not macroH2A1.2, interacts with PARP1 and XRCC1, promotes NHEJ and DDR pathways, increasing the efficiency of iPSC reprogramming. Our work might implement new strategies to improve DNA repair and reprogramming iPSC through harnessing macroH2A1 isoforms expression levels, which might open new preclinical research avenues for their practical applications.

Acknowledgments

We are grateful to the members of the Center for Translational Medicine (CTM, ICRC) for their help and support.

Funding

This research was funded by the European Regional Development Fund - Project MAGNET (No. CZ.02.1.01/0.0/0.0/15_003/0000492); by the Ministry of Health of the Czech Republic, grant nr. NV18-03-00058; and by the European Commission Horizon 2020 Framework Program (Project 856871 — TRANSTEM). The proteomic part of the study was supported by the Czech Science Foundation (project No. 19-29701L). CIISB, Instruct-CZ Centre of Instruct-ERIC EU consortium, funded by MEYS CR infrastructure project LM2018127, is gratefully acknowledged for the financial support of the measurements at the CEITEC Proteomics Core Facility. The funding sources had no role in conducting the research. P.R. is supported by a Wellcome Trust grant (208375/Z/17/Z) to J.P.M.

Conflict of Interest

The authors indicated no financial relationships.

Author Contributions

S.G.: collection and/or assembly of data, data analysis and interpretation, manuscript writing, final approval of manuscript; D.Ř.: Collection and/or assembly of data, Manuscript writing, Final approval of manuscript; T.B., G.L., Z.Z.: collection and/or assembly of data, data analysis and interpretation, final approval of manuscript; O.L.R., P.R., P.P., I.P.: collection and/or assembly of data, final approval of manuscript; I.R., M.M., J.P.M., I.K.: provision of study material, final approval of manuscript; T.M.: collection and/or assembly of data, data analysis and interpretation, provision of study material, final approval of manuscript; M.V.: conception and design, financial support, data analysis and interpretation, provision of study material, manuscript writing, final approval of manuscript.

Data Availability

The mass spectrometry proteomics data have been deposited to the ProteomeXchange Consortium via the PRIDE[82] partner repository with the dataset identifier PXD022968. RNA-Seq data were deposited in Gene Expression Omnibus with the dataset identifier GSE164396.

Supplementary Material

Supplementary material is available at *Stem Cells* online.

References

1. Hustedt N, Durocher D. The control of DNA repair by the cell cycle. *Nat Cell Biol*. 2016;19(1):1-9.

2. Jackson SP, Bartek J. The DNA-damage response in human biology and disease. *Nature*. 2009;461(7267):1071-1078.
3. Nelson BC, Dizdaroglu M. Implications of DNA damage and DNA repair on human diseases. *Mutagenesis*. 2020;35(1):1-3.
4. Takahashi K, Yamanaka S. Induction of pluripotent stem cells from mouse embryonic and adult fibroblast cultures by defined factors. *Cell*. 2006;126(4):663-676.
5. Lee AS, Tang C, Rao MS, Weissman IL, Wu JC. Tumorigenicity as a clinical hurdle for pluripotent stem cell therapies. *Nat Med*. 2013;19(8):998-1004.
6. Rocha CRR, Lerner LK, Okamoto OK, Marchetto MC, Menck CFM. The role of DNA repair in the pluripotency and differentiation of human stem cells. *Mutat Res*. 2013;752(1):25-35.
7. Turinetto V, Orlando L, Giachino C. Induced pluripotent stem cells: advances in the quest for genetic stability during reprogramming process. *Int J Mol Sci*. 2017;18(9).
8. Rodgers K, McVey M. Error-prone repair of DNA double-strand breaks. *J Cell Physiol*. 2016;231(1):15-24.
9. Luo LZ, Gopalakrishna-Pillai S, Nay SL, et al. DNA repair in human pluripotent stem cells is distinct from that in non-pluripotent human cells. *PLoS One*. 2012;7(3):e30541.
10. Allis CD, Jenuwein T. The molecular hallmarks of epigenetic control. *Nat Rev Genet*. 2016;17(8):487-500.
11. Giallongo S, Lo Re O, Vinciguerra M. Macro histone variants: emerging rheostats of gastrointestinal cancers. *Cancers*. 2019;11(5):676.
12. Giallongo S, Rehakova D, Raffaele M, et al. Redox and epigenetics in human pluripotent stem cells differentiation. *Antioxid Redox Signal*. 2020;34(4):335-349.
13. Lo Re O, Vinciguerra M. Histone MacroH2A1: a chromatin point of intersection between fasting, senescence and cellular regeneration. *Genes (Basel)*. 2017;8(12):367.
14. Buschbeck M, Hake SB. Variants of core histones and their roles in cell fate decisions, development and cancer. *Nat Rev Mol Cell Biol*. 2017;18(5):299-314.
15. Cantariño N, Douet J, Buschbeck M. MacroH2A-an epigenetic regulator of cancer. *Cancer Lett*. 2013;336(2):247-252.
16. Gaspar-Maia A, Qadeer ZA, Hasson D, et al. MacroH2A histone variants act as a barrier upon reprogramming towards pluripotency. *Nat Commun*. 2013;4:1565.
17. Barrero MJ, Sese B, Kuebler B, et al. Macrohistone variants preserve cell identity by preventing the gain of H3K4me2 during reprogramming to pluripotency. *Cell Rep*. 2013;3(4):1005-1011.
18. Khurana S, Kruhlak MJ, Kim J, et al. A macrohistone variant links dynamic chromatin compaction to BRCA1-dependent genome maintenance. *Cell Rep*. 2014;8(4):1049-1062.
19. Kim J, Oberdoerffer P, Khurana S. The histone variant macroH2A1 is a splicing-modulated caretaker of genome integrity and tumor growth. *Mol Cell Oncol*. 2018;5(3):e1441629.
20. Kim J, Sun C, Tran AD, et al. The macroH2A1.2 histone variant links ATRX loss to alternative telomere lengthening. *Nat Struct Mol Biol*. 2019;26(3):213-219.
21. Timinszky G, Till S, Hassa PO, et al. A macrodomain-containing histone rearranges chromatin upon sensing PARP1 activation. *Nat Struct Mol Biol*. 2009;16(9):923-929.
22. Borghesan M, Fusilli C, Rappa F, et al. DNA Hypomethylation And Histone Variant macroH2A1 synergistically attenuate chemotherapy-induced senescence to promote hepatocellular carcinoma progression. *Cancer Res*. 2016;76(3):594-606.
23. Lo Re O, Fusilli C, Rappa F, et al. Induction of cancer cell stemness by depletion of macrohistone H2A1 in hepatocellular carcinoma. *Hepatology*. 2018;67(2):636-650.
24. Gunn A, Stark JM. I-SceI-based assays to examine distinct repair outcomes of mammalian chromosomal double strand breaks. *Methods Mol Biol*. 2012;920:379-391.
25. Giallongo S, Lo Re O, Lochmanova G, et al. Phosphorylation within intrinsic disordered region discriminates histone variant macroH2A1 splicing isoforms-macroH2A1.1 and macroH2A1.2. *Biology (Basel)*. 2021;10(7):659.
26. Legartova S, Lochmanova G, Zdrahal Z, et al. DNA damage changes distribution pattern and levels of HP1 protein isoforms in the nucleolus and increases phosphorylation of HP1beta-Ser88. *Cells*. 2019;8(9):1097.
27. Rahimi M, Ng EP, Bakhtiari K, et al. Zeolite nanoparticles for selective sorption of plasma proteins. *Sci Rep*. 2015;5:17259.
28. Bereshchenko O, Lo Re O, Nikulenkov F, et al. Deficiency and haploinsufficiency of histone macroH2A1.1 in mice recapitulate hematopoietic defects of human myelodysplastic syndrome. *Clin Epigenetics*. 2019;11(1):121.
29. Testa G, Schaft J, van der Hoeven F, et al. A reliable lacZ expression reporter cassette for multipurpose, knockout-first alleles. *Genesis*. 2004;38(3):151-158.
30. Rappa F, Greco A, Podrini C, et al. Immunopositivity for histone macroH2A1 isoforms marks steatosis-associated hepatocellular carcinoma. *PLoS One*. 2013;8(1):e54458.
31. Pazienza V, Panebianco C, Rappa F, et al. Histone macroH2A1.2 promotes metabolic health and leanness by inhibiting adipogenesis. *Epigenetics Chromatin*. 2016;9:45.
32. Bellanti F, Iannelli G, Blonda M, et al. Alterations of clock gene RNA expression in brain regions of a triple transgenic model of Alzheimer's disease. *J Alzheimers Dis*. 2017;59(2):615-631.
33. Xu J. Preparation, culture, and immortalization of mouse embryonic fibroblasts. *Curr Protoc Mol Biol*. 2005;Chapter 28:Unit 28.1.
34. Pazienza V, Borghesan M, Mazza T, et al. SIRT1-metabolite binding histone macroH2A1.1 protects hepatocytes against lipid accumulation. *Aging (Albany NY)*. 2014;6(1):35-47.
35. Pindjakova J, Sartini C, Lo Re O, et al. Gut dysbiosis and adaptive immune response in diet-induced obesity vs. systemic inflammation. *Front Microbiol*. 2017;8:1157.
36. Chadwick BP, Willard HF. Histone H2A variants and the inactive X chromosome: identification of a second macroH2A variant. *Hum Mol Genet*. 2001;10(10):1101-1113.
37. Kovacovicova K, Skolnaja M, Heinmaa M, et al. Senolytic cocktail Dasatinib+Quercetin (D+Q) does not enhance the efficacy of senescence-inducing chemotherapy in liver cancer. *Front Oncol*. 2018;8:459.
38. Kovacovicova K, Vinciguerra M. Isolation of senescent cells by iodixanol (OptiPrep) density gradient-based separation. *Cell Prolif*. 2019;52(6):e12674.
39. Raffaele M, Kovacovicova K, Bonomini F, Rezzani R, Frohlich J, Vinciguerra M. Senescence-like phenotype in post-mitotic cells of mice entering middle age. *Aging (Albany NY)*. 2020;12(14):13979-13990.
40. Stejskal S, Stepka K, Tesarova L, et al. Cell cycle-dependent changes in H3K56ac in human cells. *Cell Cycle*. 2015;14(24):3851-3863.
41. Jueliger S, Lyons J, Cannito S, et al. Efficacy and epigenetic interactions of novel DNA hypomethylating agent guadecitabine (SGI-110) in preclinical models of hepatocellular carcinoma. *Epigenetics*. 2016;11(10):1-12.
42. Trinkle-Mulcahy L, Boulon S, Lam YW, et al. Identifying specific protein interaction partners using quantitative mass spectrometry and bead proteomes. *J Cell Biol*. 2008;183(2):223-239.
43. Hurtado-Bagès S, Guberovic I, Buschbeck M. The MacroH2A1.1—PARP1 axis at the intersection between stress response and metabolism. *Front Genet*. 2018;9:417.
44. Caldecott KW. XRCC1 protein; Form and function. *DNA Repair (Amst)*. 2019;81:102664.
45. Kang YJ, Yan CT. Regulation of DNA repair in the absence of classical non-homologous end joining. *DNA Repair (Amst)*. 2018;68:34-40.
46. Wei H, Yu X. Functions of PARylation in DNA damage repair pathways. *Genomics Proteomics Bioinformatics*. 2016;14(3):131-139.
47. Kutuzov MM, Belousova EA, Kurgina TA, et al. The contribution of PARP1, PARP2 and poly(ADP-ribosyl)ation to base excision repair in the nucleosomal context. *Sci Rep*. 2021;11(1):4849.
48. Xia W, Ci S, Li M, et al. Two-way crosstalk between BER and c-NHEJ repair pathway is mediated by Pol-β and Ku70. *FASEB J*. 2019;33(11):11668-11681.

49. Han J, Ruan C, Huen MSY, et al. BRCA2 antagonizes classical and alternative nonhomologous end-joining to prevent gross genomic instability. *Nat Commun*. 2017;8(1):1470.
50. Simara P, Tesarova L, Rehakova D, et al. Reprogramming of adult peripheral blood cells into human induced pluripotent stem cells as a safe and accessible source of endothelial cells. *Stem Cells Dev*. 2018;27(1):10-22.
51. Branzei D, Foiani M. Regulation of DNA repair throughout the cell cycle. *Nat Rev Mol Cell Biol*. 2008;9(4):297-308.
52. van Dam S, Craig T, de Magalhães JP. GeneFriends: a human RNA-seq-based gene and transcript co-expression database. *Nucleic Acids Res*. 2015;43(Database issue):D1124-D1132.
53. Bocchi R, Egervari K, Carol-Perdiguer L, et al. Perturbed Wnt signaling leads to neuronal migration delay, altered interhemispheric connections and impaired social behavior. *Nat Commun*. 2017;8(1):1158.
54. Salm EJ, Dunn PJ, Shan L, et al. TMEM163 regulates ATP-gated P2X receptor and behavior. *Cell Rep*. 2020;31(9):107704.
55. Tsai AP, Lin PB, Dong C, et al. INPP5D expression is associated with risk for Alzheimer's disease and induced by plaque-associated microglia. *Neurobiol Dis*. 2021;153:105303.
56. Singh K, Lilleväli K, Gilbert SF, et al. The combined impact of IgLON family proteins Lsamp and Neurotrimin on developing neurons and behavioral profiles in mouse. *Brain Res Bull*. 2018;140:5-18.
57. Simara P, Tesarova L, Rehakova D, et al. DNA double-strand breaks in human induced pluripotent stem cell reprogramming and long-term *in vitro* culturing. *Stem Cell Res Ther*. 2017;8(1):73.
58. Štefková K, Procházková J, Pacherník J. Alkaline phosphatase in stem cells. *Stem Cells Int*. 2015;2015:628368.
59. Lengner CJ. iPS cell technology in regenerative medicine. *Ann N Y Acad Sci*. 2010;1192:38-44.
60. Yamanaka S. Pluripotent stem cell-based cell therapy-promise and challenges. *Cell Stem Cell*. 2020;27(4):523-531.
61. Hodge DQ, Cui J, Gamble MJ, Guo W. Histone variant MacroH2A1 plays an isoform-specific role in suppressing epithelial-mesenchymal transition. *Sci Rep*. 2018;8(1):841.
62. Ruiz PD, Hamilton GA, Park JW, et al. MacroH2A1 regulation of Poly(ADP-Ribose) synthesis and stability prevents necrosis and promotes DNA repair. *Mol Cell Biol*. 2019;40(1):e00230-19.
63. Kim J, Sturgill D, Sebastian R, et al. Replication stress shapes a protective chromatin environment across fragile genomic regions. *Mol Cell*. 2018;69(1):36-47.e7.
64. Sebastian R, Hosogane EK, Sun EG, et al. Epigenetic regulation of DNA repair pathway choice by MacroH2A1 splice variants ensures genome stability. *Mol Cell*. 2020;79(5):836-845.e7.
65. Wang M, Wu W, Wu W, et al. PARP-1 and Ku compete for repair of DNA double strand breaks by distinct NHEJ pathways. *Nucleic Acids Res*. 2006;34(21):6170-6182.
66. Audebert M, Salles B, Calsou P. Involvement of poly(ADP-ribose) polymerase-1 and XRCC1/DNA ligase III in an alternative route for DNA double-strand breaks rejoining. *J Biol Chem*. 2004;279(53):55117-55126.
67. Cedeno RJ, Nakauka-Ddamba A, Yousefi M, et al. The histone variant macroH2A confers functional robustness to the intestinal stem cell compartment. *PLoS One*. 2017;12(9):e0185196.
68. Salic A, Mitchison TJ. A chemical method for fast and sensitive detection of DNA synthesis in vivo. *Proc Natl Acad Sci USA*. 2008;105(7):2415-2420.
69. Hanzlikova H, Kalasova I, Demin AA, Pennicott LE, Cihlarova Z, Caldecott KW. The Importance of Poly(ADP-Ribose) polymerase as a sensor of unligated okazaki fragments during DNA replication. *Mol Cell*. 2018;71(2):319-331.e3.
70. Wren JD, Conway T. Meta-analysis of published transcriptional and translational fold changes reveals a preference for low-fold inductions. *OMICS*. 2006;10(1):15-27.
71. Dardenne E, Pierredon S, Driouch K, et al. Splicing switch of an epigenetic regulator by RNA helicases promotes tumor-cell invasiveness. *Nat Struct Mol Biol*. 2012;19(11):1139-1146.
72. Hu Y, Chopra V, Chopra R, et al. Transcriptional modulator H2A histone family, member Y (H2AFY) marks Huntington disease activity in man and mouse. *Proc Natl Acad Sci USA*. 2011;108(41):17141-17146.
73. Haremaki T, Metzger JJ, Rito T, Ozair MZ, Etoc F, Brivanlou AH. Self-organizing neuruloids model developmental aspects of Huntington's disease in the ectodermal compartment. *Nat Biotechnol*. 2019;37(10):1198-1208.
74. Li H, Lai P, Jia J, et al. RNA Helicase DDX5 inhibits reprogramming to pluripotency by miRNA-based repression of RYBP and its PRC1-dependent and -independent functions. *Cell Stem Cell*. 2017;20(4):462-477 e466.
75. Novikov L, Park JW, Chen H, Klerman H, Jalloh AS, Gamble MJ. QKI-mediated alternative splicing of the histone variant MacroH2A1 regulates cancer cell proliferation. *Mol Cell Biol*. 2011;31(20):4244-4255.
76. Li F, Yi P, Pi J, et al. QKI5-mediated alternative splicing of the histone variant macroH2A1 regulates gastric carcinogenesis. *Oncotarget*. 2016;7(22):32821-32834.
77. Cochrane A, Kelaini S, Tsifaki M, et al. Quaking is a key regulator of endothelial cell differentiation, neovascularization, and angiogenesis. *Stem Cells*. 2017;35(4):952-966.
78. Bragança J, Lopes JA, Mendes-Silva L, Almeida Santos JM. Induced pluripotent stem cells, a giant leap for mankind therapeutic applications. *World J Stem Cells*. 2019;11(7):421-430.
79. Guhr A, Kobold S, Seltmann S, Seiler Wulczyn AEM, Kurtz A, Löser P. Recent trends in research with human pluripotent stem cells: impact of research and use of cell lines in experimental research and clinical trials. *Stem Cell Reports*. 2018;11(2):485-496.
80. Stoddard-Bennett T, Reijo Pera R. Treatment of Parkinson's disease through personalized medicine and induced pluripotent stem cells. *Cells*. 2019;8(1):80.
81. Cyranoski D. 'Reprogrammed' stem cells approved to mend human hearts for the first time. *Nature*. 2018;557(7707):619-620.
82. Perez-Riverol Y, Csordas A, Bai J, et al. The PRIDE database and related tools and resources in 2019: improving support for quantification data. *Nucleic Acids Res*. 2019;47(D1):D442-D450.